Direct solution of the Boltzmann Transport Equation in nanoscale Si devices

Kausar Banoo and Mark Lundstrom
1285 School of Electrical Engineering, Purdue University, West Lafayette, IN 47907
R. Kent Smith
PO Box 636, Bell Laboratories, Lucent Technologies, Murray Hill, NJ 07974-0636

Abstract — **We report the first direct numerical solution to the Boltzmann Transport Equation (BTE) without making any approximations about the angular shape of the distribution function or the collision integral. The mathematical and numerical techniques used for solving this problem will be discussed and shown to have the correct properties for semiconductor simulation. The applications of this method are general and will be demonstrated here, for both one-dimensional (50nm n^+-p-n^+) and two-dimensional (50nm ultra-thin body dual-gate nMOSFET) devices.**

I. INTRODUCTION

It has been recently demonstrated that when a reasonably conventional MOSFET design is scaled down to 30–60 nm, it operates in the quasi-ballistic regime [1]. This is the regime where the carriers get accelerated in critical regions of the device without much scattering [2]. The "critical region" turns out to be a low-field region of one-mean free path near the source where we expect near-equilibrium transport to take place. But, in fact, this transport is not "near-equilibrium" in the traditional drift-diffusion sense — it is "quasi-ballistic" [3]. The importance of this effect is seen in the impact on device performance and in our physical understanding of device scaling issues as we approach the end of the SIA roadmap.

Hence, as devices shrink, it becomes more important to correctly account for strong off-equilibrium and quasi-ballistic effects (among others). This work demonstrates that that can only be done by a direct numerical solution of the Boltzmann Transport Equation (BTE) in nano-scale devices. This analysis also indicates that the underlying assumptions of common macroscopic approximations of the BTE (such as drift-diffusion and hydrodynamic-type) break down when the distribution function of the carriers becomes highly asymmetric in critical regions of the device.

We begin by describing the solution of the steady-state non-degenerate BTE by using the correct mathematical and numerical techniques. This method is unlike earlier stochastic methods of solution [4] and other approximate techniques because it does not make any approximations about the angular shape of the distribution function or the collision integral. Here we present a brief discussion of the discretisation and the associated numerical issues (discretisation errors, convergence and method for solution). We then use this methodology to solve the BTE self-consistently for two typical 50nm devices (in both 1D and 2D) and study of effect of "quasi-ballistic" transport on device performance.

II. DISCRETISATION

The steady-state non-degenerate BTE is an equation in six-dimensional space $\mathcal{R}_r^3 \otimes \mathcal{R}_k^3$. Therefore, we first describe the discretisation of the BTE in momentum space and then in real space. For the purposes of this paper, we will assume a simple, spherical non-parabolic energy band with inelastic acoustic and optical (intervalley) phonon scattering and parameters calibrated to bulk Si. However, this method is not restricted to a specific band-structure because we discretise in both energy and angle in momentum space. This is done by discretising the momentum space into shells of constant energy spacing (denoted by ΔE) and further dividing the shells into spherical angle segments (denoted by $\Delta\theta = \pi/N_\theta$ and $\Delta\phi = 2\pi/N_\phi$). The grids used for the purposes of analysis in this paper are tabulated in Table 1.

N_θ, N_ϕ / ΔE	4,4	8,8
0.1 eV		1088
0.05 eV	528	2112
0.025 eV		4160

Table 1: Tabulation of grid sizes (N_k) used in this work.

The numbers refer to the total size of the grid $N_k = N_E \times N_\theta \times N_\phi$, denoting the number of points in momentum space for which we have to solve the distribution function, in each case.

After generating the grid, we perform a standard generalised box discretisation (or "control volume integration") of the BTE for all volume elements of the momentum space. The application of the method turns out to be

0-7803-6279-9/00/$10.00 © 2000 IEEE

non-trivial because of the strict conservation properties of the collision integral. However, it can be done by *converting* the volume collision integral into a *surface* integral over *all* possible scattering states and then performing a five-dimensional numerical integration of the scattering rates (for details, please see [5]). This enables us to preserve "detailed balance" (charge, momentum and energy conservation) in the collision integral that have been difficult to handle before. We then test the discrete collision term by computing its equilibrium (null) solution and

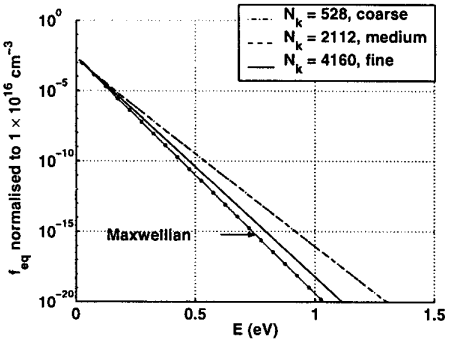

Figure 1: Equilibrium distributions for phonon scattering with increasing N_k.

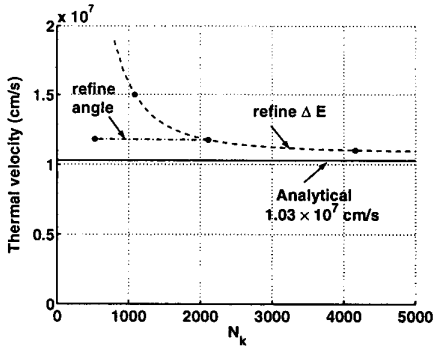

Figure 2: Thermal velocities for distributions in Fig. 1.

the corresponding thermal velocity (Figs. 1 and 2). As expected, we find that as we refine the momentum space grid, we approach the analytical solution. Note that the effect of energy refinement is more significant than angular refinement (*under equilibrium*).

The box discretisation of the field term converts it into an "upwind" matrix that preserves the direction of acceleration of the field as well as charge. Similar to the previous analysis, we test the accuracy of the discrete collision *and* field terms by computing their bulk (null) solutions for different fields and plotting velocity of the bulk distributions versus field (Fig. 3). Again, we find that as we refine N_k, we obtain the correct answer (compared to Monte Carlo bulk Si). In this case, the effect of energy as well as angular refinement is critical.

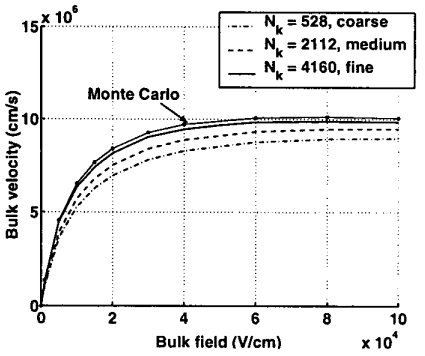

Figure 3: Bulk velocity versus field with momentum space refinement.

Finally, we include the spatial term by performing a similar box discretisation ("control volume integration") on a real space grid (represented by the number of real space elements N_x). To begin with, we test the accuracy by solving the BTE on a fixed 1D potential profile with a 20nm region of low field (-1 V/cm), 30nm region of high field (-1×10^5 V/cm) and 60 nm region of low field (1 V/cm). The description of the real space grid is given in Table 2. The momentum space grid was fixed for this analysis ($N_k = 4160$).

$\Delta x_{lo}, \Delta x_{hi}$	N_x
50Å, 5Å	76
10Å, 10Å	110
10Å, 5Å	140

Table 2: Tabulation of grid sizes (N_x) used in this work.

Fig. 4 shows the average velocity of the solutions for different N_x. We find that, by refining N_x appropriately, we obtain the correct solution compared to Monte Carlo.

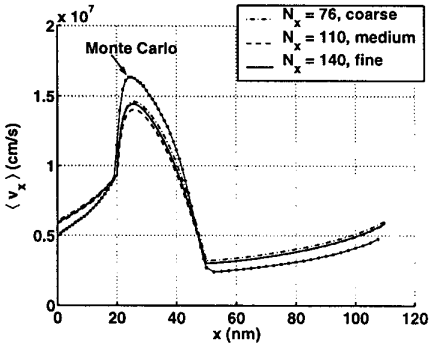

Figure 4: Average velocity for a fixed 1D potential profile with real space refinement ($N_k = 4160$ fixed).

Here, we must point out that such a complete direct discretisation of the BTE results in a *very* large matrix

equation. The number of unknowns is $N = N_x \times N_k$ and is usually $\geq 10^6$. For the first time, such a large system of equations has been solved efficiently and quickly by using a preconditioned iterative method (restarted GMRES [6]). Since the speed of solution critically depends on the preconditioner, we have devised a fast preconditioner that yields solution speeds of 35 minutes, 15 iterations for 10^6 unknowns (on a 400 MHz Ultra2). The time for solution goes as $N^{1.2}$ (Fig. 5). Furthermore, this method does not have large memory requirements to store all the elements of a $10^6 \times 10^6$ matrix because they are generated on the fly *only* when required in the matrix-vector multiplication step of the iterative method.

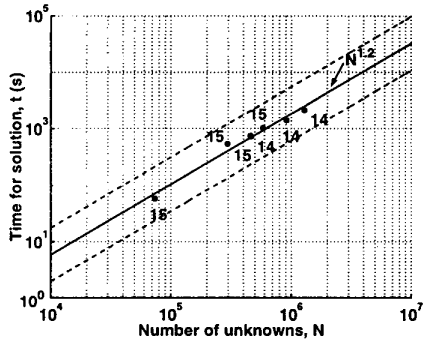

Figure 5: Time taken to solve BTE with N unknowns (numbers on the plot denote number of iterations).

Finally, we find that coupling the BTE to the nonlinear Poisson equation is extremely stable and converges in ≈ 8 iterations for a typical device (Fig. 6).

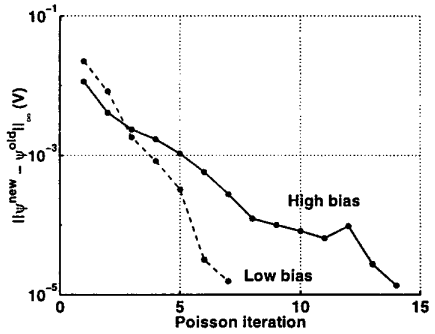

Figure 6: Convergence of BTE-Poisson iterations.

III. APPLICATIONS

We apply the above method to solve the BTE self-consistently in a 1D n^+-p-n^+ device with a 50 nm channel. This solution is then compared to the corresponding self-consistent ballistic (*i.e.* without scattering) solution at high bias. Fig. 7 shows that the average velocities of the two solutions are comparable in the low-field region near the source. This suggests that the distribution functions are highly asymmetric in the critical regions of these nanoscale devices. This concept can be measured in terms of the reflection coefficient $r_c = j^-/j^+$ [2] (Fig. 8).

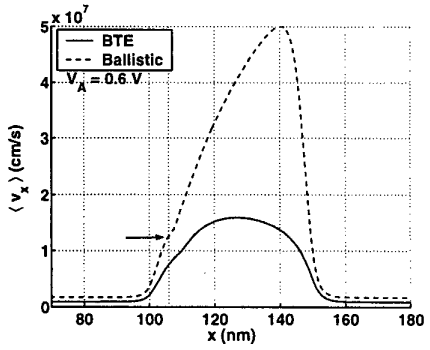

Figure 7: Average velocity (with scattering and ballistic) for n^+-p-n^+ device with 50 nm channel at 0.6V bias.

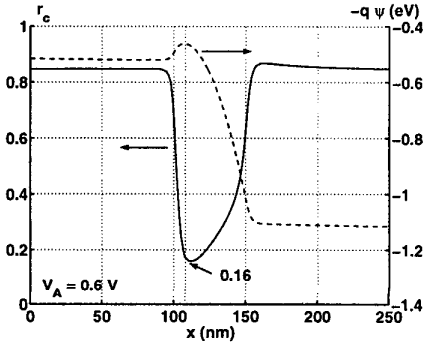

Figure 8: Reflection coefficient and potential profile for device in Fig. 7.

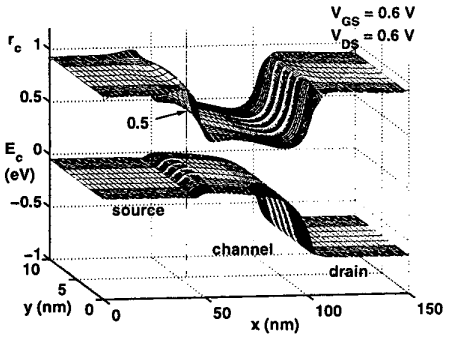

Figure 9: Reflection coefficient and conduction band profile for nMOSFET with 50 nm channel at $V_{GS} = V_{DS} = 0.6$V.

Similarly, we solve the BTE for a dual-gate ultra-thin

body 50 nm channel nMOSFET with t_{ox} = 2nm and t_{Si} = 10nm. We choose an undoped channel and adjust the V_T by using a mid-gap metal with a suitable work function. In addition, a complete definition of a 2D device requires a boundary condition on the insulating surface in terms of surface scattering [7]. We choose 6% diffusive scattering that effectively reduces the inversion layer mobility to with respect to the transverse field [8]. Fig. 9 shows that the reflection coefficient at high bias (0.6 V) drop sharply at the top of the barrier. Fig. 10 shows that the average velocity inside the device shows moderate velocity overshoot at the bias under consideration.

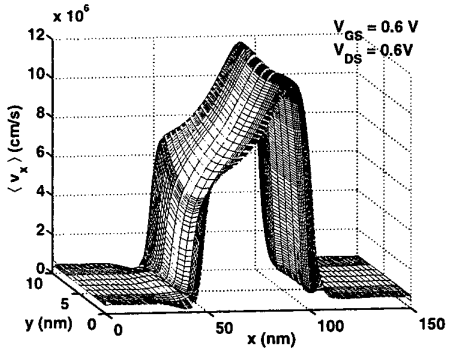

Figure 10: Average velocity for nMOSFET in Fig. 9.

IV. SUMMARY

This work shows that a direct numerical solution of the BTE is possible and provides a correct description of the effects of quasi-ballistic, velocity overshoot and non-equilibrium transport in nano-scale devices.

ACKNOWLEDGMENT

This work was supported by the NSF Distributed Center for Advanced Electronic Simulation (DesCArtES).

REFERENCES

[1] G. Timp and J. Bude *et al.*, "The ballistic nano-transistor", *in IEDM Technical Digest*, vol. 99CH36318, pp. 55–58, Electron Devices Society of IEEE, Piscataway NJ, 1999.

[2] M. S. Lundstrom, "Scattering theory of the short-channel MOSFET", *in IEDM Technical Digest*, vol. 96CH35961, pp. 387–390, Electron Devices Society of IEEE, Piscataway NJ, 1996.

[3] K. Banoo, J.-H. Rhew, M.S. Lundstrom, C.-W. Shu, and J.W. Jerome, "Simulating Quasi-Ballistic Transport in Si nanotransistors", to appear in proceedings of *Seventh International Workshop on Computational Electronics*, 2000.

[4] C. Jacoboni and L. Reggiani, "The Monte Carlo method for the solution of charge transport in semiconductors with applications to covalent materials", *Rev. Mod. Phys.*, vol. 55, pp. 645–705, 1983.

[5] K. Banoo, *to be completed*, PhD thesis, Purdue University, August 2000.

[6] Y. Saad and M. H. Schultz, "GMRES: A generalized minimal residual algorithm for solving nonsymmetric linear systems", *SIAM J. Sci. Stat. Comput.*, vol. 7, pp. 856–869, 1986.

[7] J.R. Schrieffer, "Effective carrier mobility in surface-space charge layers", *Phys. Rev.*, vol. 97, pp. 641–646, 1955.

[8] E. Sangiorgi and M. R. Pinto, "A semi-empirical model of surface scattering for Monte Carlo simulation of Silicon nMOSFETs", *IEEE Trans. Electron Devices*, vol. 39, pp. 356–361, 1992.